

Synthesis of 1,4-disubstituted-1,2,3-Triazole derivatives for investigation of inhibition and molecular docking studies against Xanthine Oxidase

Mustafa Nabeel Mirdan Mirdan¹, Guler Yagiz Erdemir¹, Samir Abbas Ali Noma², Tugba Taskin Tok^{3,4}, Burhan Ates^{5,*}, Aliye Altundas^{1,*}

¹Department of Chemistry, Faculty of Science, Gazi University, Ankara, Turkey. ²Department of Chemistry, Faculty of Arts and Science, Bursa Uludag University, Bursa, Turkey. ³Department of Chemistry, Faculty of Arts and Science, Gaziantep University, Gaziantep, Turkey.

⁴Department of Bioinformatics and Computational Biology, Institute of Health Sciences, Gaziantep University, Gaziantep, Turkey.

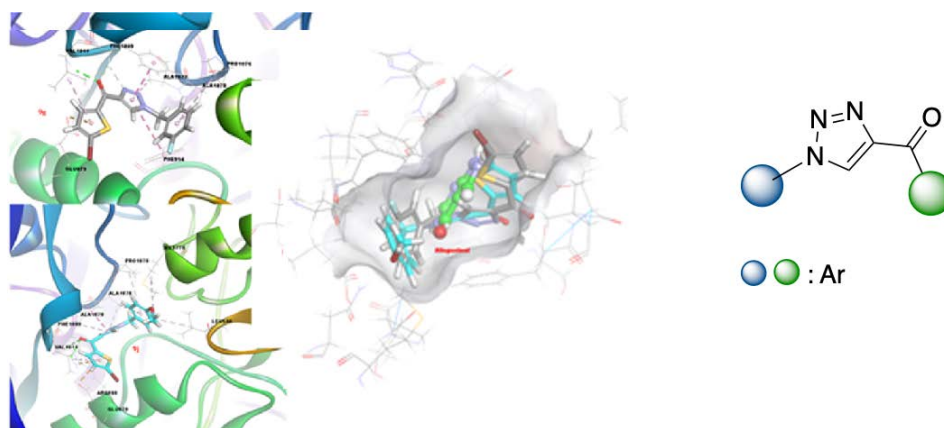
⁵Department of Chemistry, Faculty of Arts and Science, Inonu University, Malatya, Turkey

Submitted on: 08-Aug-2023, Accepted and Published on: 18-Sep-2023

Article

ABSTRACT

This study evaluates the inhibition effect of new 1,4-disubstituted-1,2,3-triazoles against Xanthine Oxidase supplemented by molecular modelling. Nine compounds of 1,4-disubstituted-1,2,3-triazoles by Sharpless's approach have been synthesized in this report. The structures of the synthesized compounds were characterized using FT-IR, ¹H and ¹³C-NMR and Mass spectroscopies. Among these synthesized molecules (5-bromothiophen-2-yl)(1-(3-



fluorobenzyl)-1H-1,2,3-triazole-4-yl)methanone (**9f**) and (5-Bromothiophen-2-yl(1-(4-methoxybenzyl)-1H-1,2,3-triazole-4-yl)methanone (**9h**) showed better activity against Xanthine oxidase (XO) compared to allopurinol. In the light of the XO inhibition results, triazoles having of ketone moiety (**9f-i**) were found to be more active than triazoles of ketone-free (**9a-e**). These results were supported by docking models. The docking calculations of the target XO with nine available compounds showed good binding energies with favourable binding interactions. These findings were particularly evident that **9f** (BE -7.29 kcal/mol) and **9h** (BE -7.59 kcal/mol) are represented encouraging higher inhibition properties towards xanthine oxidase (XO), compared to allopurinol as a reference compound. Significant binding energies and interactions obtained by performing the docking studies are demonstrated, in particular, that the compounds **9f** and **9h** may be more potential bio compounds than the positive compounds, allopurinol, and febuxostat.

Keywords: Triazole, xanthine oxidase, molecular docking, enzyme inhibition

INTRODUCTION

Xanthine oxidase, a highly sophisticated flavoprotein enzyme, is responsible for uric acid formation from purines.¹⁻³ The increase in XO level leads to the formation of peroxide and superoxide and this causes oxidative stress.⁴ The increase of the level of XO enzyme is an important factor that give rise to gout illness because the increase can lead to accumulation of uric acid. The uric acid is formed in the liver and removed with the urine.

High levels of uric acid can cause several other diseases such as metabolic syndrome.⁵ The increase in the free radical and reactive oxygen species (FR&ROS) levels coming from high levels of XO can cause diverse pathological states including inflammation, cancer, metabolic disorders, and chronic obstructive pulmonary disease.⁶ To overcome these diseases, XO inhibition could minimize the production of FR & ROS and get a benefit for treatment.⁷ There are several studies in the literature on XO inhibitors with a better pharmacological profile and fewer side effects than allopurinol.^{8,9} Studies of allopurinol revealed that the modification of the purine ring is crucial to its bioactivity.¹⁰ Allopurinol is used as an XO inhibitor and plays an active role in the treatment of gout in recent years. However, allopurinol and its analogues are stated to cause disruptions in the mechanism of action.¹¹ Based on these findings, diverse XO inhibitors

*Corresponding Author: Dr. Burhan ATEŞ; Dr. Aliye ALTUNDAS
Email: burhan.ates@inonu.edu.tr (BA), aaltundas@gazi.edu.tr (AA)



comprising different five-member heterocyclic scaffolds (triazoles, imidazoles, etc.) were explored and proved to improve bioactivities.¹² In these perspectives, 1,2,3-Triazoles and their derivatives attained significant attention in the field of medicinal chemistry due to their diverse biological properties such as anti-tumour, anti-cancer, anti-TB, anti-HIV, etc.¹³⁻²¹ In addition, the research is going on to develop new 1,2,3-triazoles for the development of new drugs and therapeutic agents for various diseases.^{22,23} It is seen that among the 1,2,3-triazoles derivatives, especially the derivatives at the 4-position on this ring have attention due to strong interactions with enzymes in the recent studies.^{24,25} Recently, it is indicated that these compounds containing the azole ring have a better XO inhibitory effect than allopurinol.²⁶⁻²⁸

MATERIALS AND METHODS

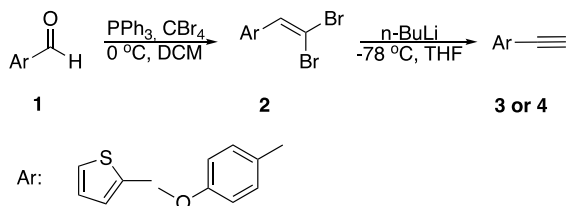
Experimental

Chemicals

The reagents used were obtained from companies such as Merck, Sigma, Fluka. Analytical purity was used for purification. Dry tetrahydrofuran was distilled immediately before synthesis. Reactions were monitored with silica-filled TLC plates attached to an alumina layer (SiO₂, Merck 60 F254). For column chromatography, silica gel (Merck60, particle size 0.040–0.063 mm) was used. For structure characterisation, functional group analyses were performed by Fourier transform infrared (FTIR), which is Bruker FTIR spectrometer. and proton (¹H) and carbon (¹³C) analyses were performed by Bruker spectrometer 300 MHz and 75 MHz with tetramethylsilane (TMS) as the internal standard, respectively. For High Resolution Mass Spectroscopy (HRMS), which is the other supporting structure analysis, service was procured from Agilent Technologies, 6224 TOF LC/MS analysis. Melting points were recorded with STUART (SMP-30) device.

Synthesis of Compound 3 and 4

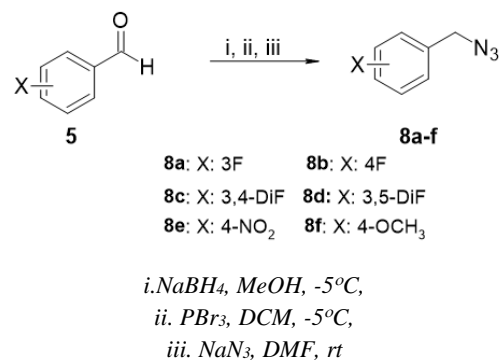
A solution of the dibromo vinyl compound (1.0 equiv.) in dry THF (30.0 mL) was stirred at -78 °C under an argon atmosphere for 20 minutes. Then *n*-BuLi (1.6 M solution in pentane) (5.0 equiv.) was added to the mixture for 1.5 h. at -78 °C. The reaction mixture was quenched with saturated ammonium chloride solution (5.0 mL) and THF was removed under reduced pressure. The mixture was diluted with H₂O (20.0 mL) and extracted with ethyl acetate (20 mL × 3). The combined ethyl acetate phase was washed with brine, dried over anhydrous Na₂SO₄, filtered and removed under reduced pressure. The residue was purified by column chromatography on SiO₂ (EtOAc/Hex; 1:4) to give the target compounds.²⁹



Scheme 1. Synthesis of arylacetylene derivatives

Synthesis of azido methyl derivatives from aldehydes

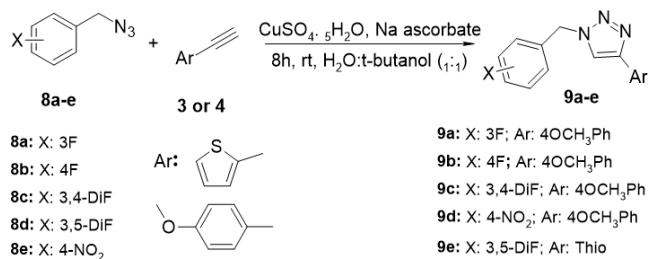
Benzyl azides were obtained in 3 steps following literatures.³⁰⁻³²



Scheme 2. Synthesis of azidobenzyl derivatives

Click reaction procedure for triazoles 9a-e synthesis

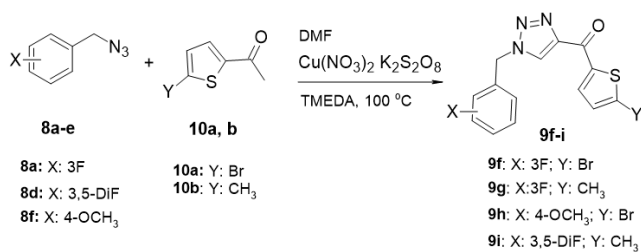
Target *N*-benzyl-4-(aryl-2-yl)-1*H*-1,2,3-triazoles (**9a-e**), were prepared by dissolving 1-ethynyl-4-methoxybenzene (**4**) or 2-ethynylthiophene (**3**) (1 equiv.) in the mixed solvent of tert-butanol and water (6 mL; 1:1) with various substituted azides (1 equiv.). Copper sulfate pentahydrate (CuSO₄·5H₂O) (0.35 equiv.) and sodium ascorbate (0.35 equiv.) were mixed and then added to the reaction medium as catalysts. The reaction mixture was stirred for 8 h at room temperature. The reaction was monitored by TLC. After the end of the reaction, the mixture was poured into brine, extracted with DCM (50 mL), and dried over Na₂SO₄. The organic phase was evaporated by vacuum. The residue was purified by flash column chromatography on silica gel eluting with hexane and EtOAc to give the corresponding product **9a-e**.³³⁻³⁶



Scheme 3. Synthesis of *N*-benzyl-4-(aryl-2-yl)-1*H*-1,2,3-triazoles

Synthesis of 9f-i

The solution of substitute-thiophene ketone **10a-b** (1 equiv.) in DMF (1 mL) was added slowly to a mixture of benzyl azide **8a**, **8d** and **8f** (1 equiv.), Cu(NO₃)₂ (0.2 equiv.), K₂S₂O₈ (3.0 equiv.), and TMEDA (0.2 eq.). The mixture was stirred at 100 °C. Upon completion of the reaction, Na₂CO₃ (aq) (10 mL) was added then extracted with EtOAc (3 × 5 mL). The combined organic extracts were dried over anhydrous Na₂SO₄, filtered and concentrated under reduced pressure. The residue was purified by flash column chromatography on silica gel eluting with hexane and EtOAc to give the corresponding product **9f-i**.³⁷



Scheme 4. Synthesis of triazolylthiophenylmethanone derivatives

1-(3-Fluorobenzyl)-4-(4-methoxyphenyl)-1H-1,2,3-triazole

(9a): Solid, m.p: 145 °C³⁵, yield: 31%. IR ν_{\max} (cm⁻¹): 3105, 2916, 1617, 1501, 1458, 1027. ¹H-NMR (δ (ppm), CDCl₃): 7.73 (d, J = 8.8 Hz, 2H), 7.67 (s, 1H), 7.35 (m, 1H), 7.07 (m, 1H), 7.04 (m, 1H), 7.00 (m, 1H), 6.94 (d, J = 8.8 Hz, 2H), 5.55 (s, 2H), 3.82 (s, 3H). ¹³C-NMR (δ (ppm), CDCl₃): 163.1, 159.7, 148.6, 137.3, 130.8, 127.1, 123.6, 123, 119, 115.8, 115, 114.3, 55.4, 53.5. HRMS (TOF): m/z calcd for C₁₆H₁₄FN₃O: 283.3064 found: 284.1204 [M+H]⁺

1-(4-Fluorobenzyl)-4-(4-methoxyphenyl)-1H-1,2,3-triazole

(9b): Solid, m.p: 157 °C³⁶, yield: 93%. IR ν_{\max} (cm⁻¹): 3135, 2926, 1607, 1502, 1458, 1222. ¹H-NMR (δ (ppm), CDCl₃): 7.72 (d, J = 8.8 Hz, 2H), 7.57 (s, 1H), 7.30 (dd, J = 8.6, 5.3 Hz, 2H), 7.08 (t, J = 8.6 Hz, 2H), 6.94 (d, J = 8.8 Hz, 2H), 5.65 (s, 2H), 3.82 (s, 3H). ¹³C-NMR (δ (ppm), CDCl₃): 163, 159.8, 148.2, 130.8, 130, 127, 123.3, 118.5, 116.3, 114, 55.5, 53.6. HRMS (TOF): m/z calcd for C₁₆H₁₄FN₃O: 283.3064 found: 284.1207 [M+H]⁺

1-(3,4-Difluorobenzyl)-4-(4-methoxyphenyl)-1H-1,2,3-triazole

(9c): Solid, m.p: 160 °C, yield: 37%. IR ν_{\max} (cm⁻¹): 3128, 2962, 1610, 1501, 1434, 1030. ¹H-NMR (δ (ppm), CDCl₃): 7.73 (d, J = 8.6 Hz, 1H), 7.61 (s, 1H), 7.22 (m, 3H), 7.00 (m, 3H), 6.93 (d, J = 8.6 Hz, 1H), 5.65 (s, 2H), 3.82 (s, 3H). ¹³C-NMR (δ (ppm), CDCl₃): 159.9, 157.3, 150.8, 146.6, 132.7, 127.2, 126.3, 124.3, 123.1, 117.3, 114.4, 55.5, 53.2. HRMS (TOF): m/z calcd for C₁₆H₁₃F₂N₃O: 301.2968 found: 302.1115 [M+H]⁺

1-(4-Methoxyphenyl)-4-(4-nitrobenzyl)-1H-1,2,3-triazole

(9d): Solid, m.p: 140 °C³⁵, yield: 28%. IR ν_{\max} (cm⁻¹): 3088, 2956, 1613, 1501, 1454, 1027. ¹H-NMR (δ (ppm), CDCl₃): 8.22 (d, J = 8.4 Hz, 2H), 7.73 (d, J = 8.4 Hz, 2H), 7.67 (s, 1H), 7.43 (d, J = 8.4 Hz, 2H), 6.94 (d, J = 8.5 Hz, 2H), 5.6 (s, 2H), 3.8 (s, 2H). ¹³C-NMR (δ (ppm), CDCl₃): 160, 148.7, 148.2, 142, 128.7, 127.2, 122.9, 119, 114.4, 55.5, 53.3. HRMS (TOF): m/z calcd for C₁₆H₁₄N₄O₃: 310.3130 found: 311.1156 [M+H]⁺

1-(3,5-Difluorobenzyl)-4-(thiophen-2-yl)-1H-1,2,3-triazole

(9e): Solid, m.p: 135-140 °C, yield: 71%. IR ν_{\max} (cm⁻¹): 3125, 3068, 1600, 1511, 1461. ¹H-NMR (δ (ppm), CDCl₃): 7.67 (s, 1H), 7.33 (d, 2H), 7.08 (dd, 1H), 6.8 (d, 3H), 5.6 (s, 2H). ¹³C-NMR (δ (ppm), CDCl₃): 163.5, 163.4, 138.3, 138.2, 138.1, 130.6, 127.9, 125.5, 124.6, 111.1, 104.6, 53.7. HRMS (TOF): m/z calcd for C₁₃H₉F₂N₃S: 277.2928 found: 278.0570 [M+H]⁺

(5-bromothiophen-2-yl)(1-(3-fluorobenzyl)-1H-1,2,3-triazole-4-yl)methanone

(9f): Solid, m.p: 150 °C, yield: 31%. IR ν_{\max} (cm⁻¹): 3111, 2952, 2853, 170, 1613, 1527, 1451. ¹H-NMR (δ (ppm), CDCl₃): 8.37 (d, 1H), 8.09 (s, 1H), 7.37 (td, 1H), 7.10 (d, 1H), 7.01 (dd, 2H), 6.93 (d, 1H), 5.6 (s, 2H). ¹³C-NMR

(δ (ppm), CDCl₃): 175.8, 163.2, 147.8, 145, 136.7, 136.0, 131.7, 131.3, 127.8, 124.8, 124.0, 116.5, 115.5. HRMS (TOF): m/z calcd for C₁₄H₉FBrN₃OS: 366.2084 found: 365.9729 [M-H]⁺

1-(3-Fluorobenzyl)-1H-1,2,3-triazole-4-yl(5-

methylthiophen-2-yl)methanone (9g): Solid, m.p: 155 °C, yield: 34%. IR ν_{\max} (cm⁻¹): 3121, 3068, 1604, 1531, 1491, 1438.

¹H-NMR (δ (ppm), CDCl₃): 8.56 (d, 1H), 8.17 (s, 1H), 7.37 (td, 1H), 7.09 (dd, 1H), 7.02 (dt, 2H), 6.89 (d, 1H), 5.6 (s, 2H), 2.37 (s, 3H). ¹³C-NMR (δ (ppm), CDCl₃): 176.7, 163.2, 151.6, 148.4, 140, 137.3, 136.2, 131.1, 127.6, 127.5, 123.9, 116.4, 115.4, 53.9, 14.6. HRMS (TOF): m/z calcd for C₁₅H₁₂FN₃OSNa⁺: 324.06003 found: 324.0577 [M+Na]⁺

(5-Bromothiophen-2-yl)(1-(4-methoxybenzyl)-1H-1,2,3-

triazole-4-yl)methanone (9h): Solid, m.p: 168 °C, yield: 82%. IR ν_{\max} (cm⁻¹): 3125, 2938, 2841, 1700, 1634, 1534, 1406, 1046.

¹H-NMR (δ (ppm), CDCl₃): 8.45 (d, 1H), 8.08 (s, 1H), 7.28 (d, J = 8.7 Hz, 2H), 7.18 (d, 1H), 6.92 (d, J = 8.7 Hz, 2H), 5.6 (s, 2H). ¹³C-NMR (δ (ppm), CDCl₃): 176, 160.4, 149.7, 147.5, 136.6, 131.6, 130.2, 127.5, 125.6, 124.6, 114.9, 55.5, 54.3. HRMS (TOF): m/z calcd for C₁₅H₁₂BrN₃O₂SNa⁺: 399.9726 found: 399.9753 [M+Na]⁺

(1-(3,5-Difluorobenzyl)-1H-1,2,3-triazole-4-yl)(5-

methylthiophen-2-yl)methanone (9i): Solid, m.p: 168-171 °C, yield: 69%. IR ν_{\max} (cm⁻¹): 3121, 3068, 2926, 2853, 1736, 1600,

1531, 1438. ¹H-NMR (δ (ppm), CDCl₃): 8.48 (s, 1H), 8.11 (s, 1H), 7.17 (s, 1H), 6.77 (s, 3H), 5.6 (s, 2H), 2.37 (s, 3H). ¹³C-NMR (δ (ppm), CDCl₃): 176.6, 163.6, 163.4, 151.8, 148.6, 140.1, 138.1, 137.4, 127.6, 124.9, 111.3, 104.8, 53.5, 16.4. HRMS (TOF): m/z calcd for C₁₅H₁₁F₂N₃OSNa⁺: 342.0483 found: 342.0507 [M+Na]⁺

In vitro Assay of XO Inhibitory Effects

Different triazole compounds were investigated for the inhibition effects on XO by observing the decrease in the uric acid level. The XO activity was evaluated by observing the increase in absorbance of uric acid levels at 294 nm, which was caused by the conversion of xanthine to uric acid. The decrease in uric acid generation was used to evaluate the catalyzed reaction for XO inhibition. To begin the reaction, XO (0.2 U), PBS (50 mM, pH 7.4), varied quantities of investigated compounds, and xanthine (1 mM) were added to the reaction mixture. Before adding the xanthine, the reaction mixture was incubated at 37 °C for 10 minutes. The activity was detected by Shimadzu UV-1601 at wavelength 294 nm. Allopurinol was used as a positive control. Then the IC₅₀ of XO enzyme was found in terms of the decrease in uric acid formation as compared to the formation in the absence of an inhibitor. The IC₅₀ was calculated as the following:

$$\text{Inhibition (\%)} = \frac{(A - B)}{A} \times 100$$

Where *A* is the absorbance without the tested compound and *B* is the absorbance with the tested extract.

Molecular Docking Procedures

The binding of novel compounds **9a-i** to XO as a target was searched using the one of in silico method, molecular docking simulation with AutoDock Vina.^{38,39} The respective compounds were sketched and done geometry optimization at DFT/B3LYP/6-31G* level of Gaussian 09.⁴⁰ Afterwards, the target XO (pdb: 3NVY) was acquired from the protein data bank database.⁴¹ Autodock Tools 1.5.7 was used to prepare and determine the binding site of the target XO. The grid size of the target enzyme is $40 \times 40 \times 40 \text{ \AA}^3$ x, y, z coordinates by taking macromolecule to the center in 0.375 \AA grid spacing. In the docking calculations, 200 conformations for each compound were left flexible, while the current enzyme was held rigid. The lowest binding energy conformers and two-dimensional (2D) interactions were chosen from 10 top ranked poses. UCSF Chimera⁴² and Discovery Studio 3.5⁴³ were also utilized for visualization of the best-docked pose and 3D target-ligand interactions in the docking studies.

RESULT AND DISCUSSION

The target compounds were synthesized after several reaction steps as indicated Scheme 1, Scheme 2, Scheme 3 and Scheme 4. The structures of the synthesized compounds were characterized using FT-IR, ¹H and ¹³C-NMR and Mass spectroscopies (Supplementary data). As a starting point, in Scheme 1 and Scheme 2, 1-ethynyl-4-methoxybenzene or 2-ethynylthiophene and substitute azido methyl were respectively synthesized as to literatures.²⁷⁻³⁰ Then these compounds, **3** or **4** and **8a-e**, were used as the main synthetic backbone to synthesize target compounds **9a-i** using Click Chemistry as like Sharpless et al. Then, the biological studies containing of XO inhibition were investigated by UV-vis absorption spectroscopy against the reference drug, Allopurinol.

1-Ethynyl-4-methoxybenzene (**3**) and 2-ethynylthiophene (**4**) were synthesized in two steps with Corey Fuchs method for their use in click chemistry according to literature. Structures of this compound were elucidated using FTIR analysis method. In the IR spectra, there is ν ($-\text{C}\equiv\text{C}-$) stretching at $2150\text{-}2200 \text{ cm}^{-1}$ supporting the formation of alkyne. The synthesis of the obtained benzyl azides was carried out in the light of literature data. As with alkynes, the structures of benzyl azides were elucidated by FTIR spectroscopy. The specific stretching band of benzyl azides (**8a-f**) at 2090 cm^{-1} in the IR spectra was evidence that these derivatives were synthesized. Derivatives containing triazole ring (**9a-i**) have been obtained from the [3 + 2] cycloaddition reaction of synthesized alkynes and azides. Structures of derivatives were characterized at using FTIR, ¹H, ¹³C NMR and HRMS-TOF, respectively. In the FTIR spectra of **9a-i** derivatives, the specific stretching band of alkynes and benzyl azides were observed at $2150\text{-}2200$ and 2090 cm^{-1} , respectively, disappeared and specific stretching band of synthesized 1,4-disubstituted-1,2,3-triazole derivatives were observed at about $3100\text{-}3150 \text{ cm}^{-1}$.

All target compounds **9a-i** were analyzed in the ¹H NMR and ¹³C APT NMR in CDCl₃ solvent. For **9a-d** derivatives, the range of 3.83-4.00 ppm (s, 3H) belongs to $-\text{OCH}_3$ and of 5.85-5.62 ppm (s, 2H) belongs to benzylic methylene. And in the **9a-d**

derivatives, the AA'XX' system of *para*-methoxybenzene ring protons can be seen at δ of 6.93 ppm (quasi d, $J = 8.6\text{-}8.8 \text{ Hz}$, 2H) for hydrogen atoms next to the methoxy group (AA' part), while the XX' part appear at δ of 7.73 ppm (quasi d, $J = 8.6\text{-}8.8 \text{ Hz}$, 2H). Hydrogen atoms of the thiophene ring on **9e-i** resonate at δ of 7.50-7.00 ppm different than **9a-d** derivatives. Lastly, the hydrogen atom of the triazole ring appears at δ range of 7.60-8.05 ppm as a singlet (s, 1H). It had been observed that the ¹³C-APT NMR spectra of the compounds are compatible with the structure as in ¹H NMR. From ¹³C APT NMR spectra data, carbon signal of the compound **9a-i** the $-\text{OCH}_3$ and $-\text{CH}_2-$ observed respectively, at around 60 ppm and almost 55 ppm and the signals at $\delta = 125\text{-}119 \text{ ppm}$ and $\delta = 160\text{-}147 \text{ ppm}$, showed the carbon C-5 and C-4 of the triazole moiety, respectively.

The *in vitro* inhibitory impact of triazole on serum bovine XO was assessed by a rise in the generation of uric acid levels at 294 nm. Increased XO levels cause many cancer types owing to an increase in ROS generation.⁴⁴ As a result, inhibiting XO decreases the formation of uric acid and ROS. Allopurinol is a purine-like molecule that is commonly utilized as an XO inhibitor. Nevertheless, because of allopurinol has a similarity of the purine metabolite, this allopurinol inhibitor produces significant adverse effects in purine metabolism. Febuxostat is the first chemical of an emerging family of antihyperuricemic medicines known as non-purine selective xanthine oxidase inhibitors. However, several studies have been conducted in order to develop more powerful non-purine XO inhibitors.⁴⁵⁻⁴⁷ In this study, we investigated the inhibitory characteristics of triazoles on the activity of XO and discovered that the IC₅₀ values ranged from 0.93 to 2.07 μM as summarized in Table 1. The IC₅₀ value of allopurinol, a commonly used medication, was determined as 3.32 μM . *In vitro* activity tests on these triazole compounds revealed that all triazole compounds performed better as xanthine oxidase inhibitors than allopurinol. Among to **9a-i** derivatives, **9a-d** compounds contain methoxyphenyl ring and **9e** contains thiophenyl ring at the 4-position of triazole ring, whereas **9f-i** compounds contain a substituted thiophenylmethanone. Through biochemical investigation, one observed that compounds of **9f** and **9h** have higher IC₅₀ values compared to the other derivatives. When the XO enzyme inhibitions of **9a-e** derivatives were evaluated within themselves **9d** has the highest inhibition value of the derivative, which bears a strongly electron-withdrawing $-\text{NO}_2$ group on the benzyl ring. However, when the activity of the thiophene ring was examined directly instead of the methoxyphenyl ring, it was seen that the activity did not change at a significant rate. Among these derivatives, the ability of the oxygen atom in the methoxy group to hydrogen bond with the hydrogen atom in the enzyme is higher than the ability of the sulfur atom in the thiophene ring in the **9e** derivative to make hydrogen bonding. Thus, 4-OMephenyl ring may have caused an increase in the enzyme inhibition of the structure.

When the activity measurements of **9f-i** derivatives containing substituted thiophene ring are examined, it is seen that **9f** and **9h** compounds have the highest inhibition activities compared to other derivatives. The compound **9f** which has a bromide atom at

the thiophene ring may be cause a further increase of interaction of enzyme center as compared to other compounds. According to the results of this study it was predicted that XO enzyme inhibition would be increased if the electron-withdrawing atom or groups contain in these compounds. Especially, among all of the derivatives of **9f** and **9h** proved to show the most potent enzyme inhibitory activity.

For determining the inhibition type of the compounds, **9f** was chosen due to the most potent inhibitor. According to inhibition data, the Lineweaver–Burk plok was prepared and given in Figure 2. These results prove **9f** has competitive inhibition properties against XO. The kinetic studies of the inhibition mechanism allowed a definition due to allopurinol and febuxostat acting as competitive inhibitors against XO.⁴⁸ These triazole derivatives having very close structure from febuxostat exhibited similar inhibition type.

In a recent study, 5-benzyl-3-pyridyl-1*H*-1,2,4-triazole exhibited the IC₅₀ for XO in the range from 0.16 to 12.70 μM⁴⁹ and in another study, dimethyl *N*-benzyl-1*H*-1,2,3-triazole-4,5-dicarboxylate and (*N*-benzyl-1*H*-1,2,3-triazole-4,5-diyl) dimethanol derivatives were reported that the IC₅₀ value range were 0.73–1.71 μM.⁵⁰ According to our results, especially, among all these triazole derivatives of **9f** and **9h** proved to be show the most potent enzyme inhibitory activity and may be a good alternative for XO inhibition.

Table 1. IC₅₀ values of **9a-i** derivatives on XO activity.

Code of synthesized derivatives	IC ₅₀ (μM)	R ²
9a	1.95 ± 0.013	0.998
9b	1.58 ± 0.030	0.989
9c	2.07 ± 0.075	0.987
9d	1.41 ± 0.042	0.986
9e	1.57 ± 0.014	0.996
9f	0.93 ± 0.020	0.975
9g	1.51 ± 0.027	0.962
9h	0.99 ± 0.043	0.995
9i	1.98 ± 0.073	0.975
Allopurinol	3.32 ± 0.029	0.978

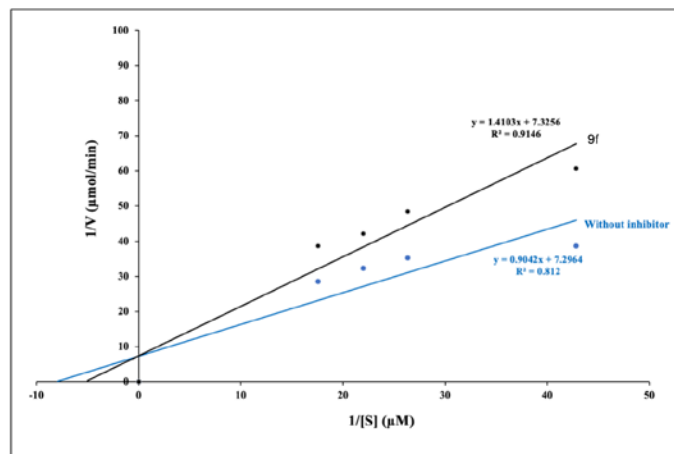


Figure 1. The inhibition type of triazole derivative (**9f**).

There are many literature reports in which new thiazole derivatives have been evaluated by computational studies as well as experimental studies.⁵¹⁻⁵⁴ In this study, thiazole derivatives synthesized using the same approach were supported by molecular docking studies. New generic compounds, whose biological activities have been studied, were observed at the molecular level through molecular docking studies. Under this perspective, the structure and activity relationships of the relevant compounds with the target were examined and evaluated. The interactions between novel 1,2,3-triazole derivatives (**9a-i**) as ligands and XO protein as target is crucial to understanding the binding affinity of ligands in the chosen target medium. In this visualized analysis, it was found that all compounds bound better to the target enzyme than a positive compound, allopurinol. This case summarized in **Table 1** numerically supports the binding energy of all compounds. Meanwhile, there is a relationship between binding energy values and biological inhibition values (Table 2 and Figure 3). They show the same tendency not in numerical values, but in their orientation, and show a harmonious and parallel relationship with each other. The relationship between XO and allopurinol is given in **Figure S 41**. Besides allopurinol, the febuxostat compound created a binding energy of -5.82 kcal/mol when we analyzed it on the relevant target computationally. Febuxostat, 2-[3-cyano-4-(2-methylpropoxy)phenyl]-4-methyl-1,3-thiazole-5-carboxylic acid structure has a larger surface area than allopurinol structure. It carries out hydrogen bonds with Asn768, Arg880, Ser876, and Phe1009 in the active site of the target enzyme, and alkyl and π-alkyl type hydrophobic interactions with Leu648 and Phe649 residues (**Figure S42** and **Table S10**). Potent compounds

Table 2. The binding energy values for the compounds (**9a-i**) and allopurinol* as a positive compound, towards XO.

Name	Binding Energy (kcal/mol)	IC ₅₀ (μM)
9a	-6.94	1.95
9b	-6.77	1.58
9c	-6.88	2.07
9d	-6.43	1.41
9e	-6.24	1.99
9f	-7.29	0.93
9g	-7.07	1.51
9h	-7.59	0.99
9i	-6.75	1.98
Allopurinol	-6.10	3.32
Febuxostat	-5.82	-

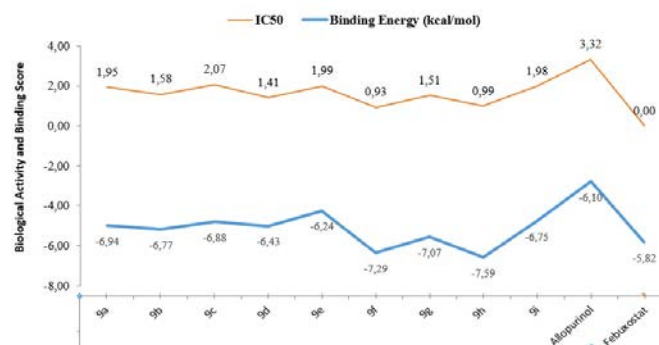


Figure 2. Relationship of binding energy values versus biological activity values (IC₅₀) of the compounds (**9a-i**) and allopurinol.

(9f and 9h) show higher binding affinity with the target than both control compounds.

Moreover, the two- and three-dimensional images of compounds 9h and 9f, which are the top of the compounds discussed, visualized using Discovery Studio 3.5 as illustrated in Figure 3. The best compound, 9h with a binding energy of -7.59 kcal/mol is makes three hydrogen bonds with Arg880 (2.839 Å and 2.482 Å) and Phe1009 (1.878 Å) amino acids; two electrostatic interactions with Arg880 (3.633 Å) and Glu879 (3.513 Å), and also eight hydrophobic interactions including pi-pi-stacked, alkyl and pi-alkyl interactions with Phe1009 (4.208 Å), Leu648 (4.237 Å), Met770 (5.152 Å), Ala1078 (3.897 Å and 5.333 Å), Ala1079 (4.206 Å), Pro1076 (4.692 Å) and Val1011 (4.743 Å) residues in the binding site of the target enzyme.

The second one, compound 9f with a binding energy of -7.29 kcal/mol is docked with Val1011 (2.250 Å), Phe1009 (2.403 Å and 2.387 Å) via hydrogen bonds; Glu879 (3.485 Å) via electrostatic interaction, and also Phe1009 (3.675 Å), Phe914 (5.837 Å), Ala1079 (4.430 Å), Pro1076 (5.413 Å), Ala1078 (4.482 Å) and Val1011 (4.230 Å) residues in the XO, via hydrophobic interactions.

In addition, Table S10 and Table S11 in the supporting information section contains the docking results of the compounds 9a-i as well as the bond distance between them, as well as potential interactions (hydrogen bonds, electrostatic, hydrophobic bonds) compounds and XO.

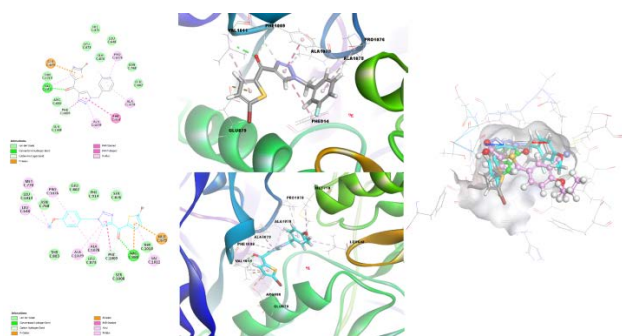


Figure 3. 2D and 3D docked pose of the compound 9f (default color, stick form), 9h (cyan color, stick form) and allopurinol (green color, ball and stick form), febuxostat (light pink color, ball and stick form), showing interaction with XO.

The two best compounds (9h and 9f), whose images and interactions we have mentioned, interact better with the target than the reference compound because the positive compound (allopurinol) interacts with Ser876 (2.949 Å), Glu879 (2.224 Å) and Arg880 (2.706 Å) amino acids by hydrogen bonding and with Phe914 (4.447 Å and 5.663 Å), Phe1009 (4.797 Å), Ala1078 (5.0971 Å) and Ala1079 (5.209 Å) residues in the target enzyme by hydrophobic interactions. The most important part here is that the electron-donating methoxy group is attached at the 4th position of the phenyl ring of the compound 9h structure and the presence of a fluorine atom in the 3rd position of the phenyl ring in the compound 9f has shown the dominant effect on the XO target and biological activities of the related compounds. In addition to these, the size of the topological surface areas of the

relevant compounds in the active region of the target against positive compound is also important.

CONCLUSION

In brief, this study contains synthesis of 1,4-disubstituted-1,2,3-triazole motifs, these motifs investigation of XO enzyme inhibition and docking studies. The structure of new compounds were synthesized by Sahrpless method and their structures characterized by using FT-IR, ¹H-NMR, ¹³C-NMR and HRMS-TOF spectroscopic techniques. The characterization data were consistent with the builds of compounds. The new triazole compounds were used to determine the efficient inhibition against XO enzymes. All synthesized 1,2,3-triazole analogues (9a-i) exerted micromolar inhibitory activities against XO. Especially, 9f and 9h manifested excellent potency against XO with IC₅₀ of 0.93 ± 0.020 and 0.99 ± 0.043. Among triazole cores, especially compounds of thiophene ring were excellent inhibition effect. Significant binding energies and interactions obtained by performing the docking studies are demonstrated, in particular, that the compounds 9f and 9h may be more potential bio compounds than the positive compounds, allopurinol, and febuxostat.

ACKNOWLEDGMENTS

The authors also thank Esin Akı Yalcin and the research group for technical assistance.

Conflict of Interest: None

REFERENCES AND NOTES

1. M. Boban, G. Kocic, S. Radenkovic, R. Pavlovic, T. Cvetkovic, M. Deljanin-Ilic, S. Ilic, S. M. D. Bobana, B. Djindjic, D. Stojanovic, D.T. Sokolovic. Circulating purine compounds, uric acid, and xanthine oxidase/dehydrogenase relationship in essential hypertension and end stage renal disease. *Renal Failure* **2014**, 36, 613-618.
2. T. Zhang, Y. Lv, Y. Lei, D. Liu, Y. Feng, J. Zhao, S. Chen, F. Meng, S. Wang. Design, synthesis and biological evaluation of 1-hydroxy-2-phenyl-4-pyridyl-1H-imidazole derivatives as xanthine oxidase inhibitors. *European journal of medicinal chemistry* **2018**, 146, 668-677.
3. P. A. L. Pacher, A. Nivorozhkin, C. Szabó. Therapeutic effects of xanthine oxidase inhibitors: renaissance half a century after the discovery of allopurinol. *Pharmacological reviews* **2006**, 58, 87-114.
4. Z. Smelcerovic, A. Veljkovic, G. Kocic, D. Yancheva, Z. Petronijevic, M. Anderluh, A. Smelcerovic. Xanthine oxidase inhibitory properties and anti-inflammatory activity of 2-amino-5-alkylidene-thiazol-4-ones. *Chemico-biological interactions* **2015**, 229, 73-81.
5. R. Hille. Structure and function of xanthine oxidoreductase *European journal of inorganic chemistry* **2006**, 10, 1913.
6. S. Pereira, J. Almeida, A. O. Silva, M. Quintas, O. Candeias, F. Freitas. Fatal liver necrosis due to allopurinol. *Acta medica portuguesa* **2018**, 11, 1141-1144.
7. H. Horiuchi, M. Ota, S. I. Nishimura, H. Kaneko, Y. Kasahara, T. Ohta, K. Komoriya. Allopurinol induces renal toxicity by impairing pyrimidine metabolism in mice. *Life Sciences* **2000**, 66, 2051-2070.
8. J.X. Zhu, Y. Wang, L.D. Kong, C. Yang, X. Zhang. Effects of Biota orientalis extract and its flavonoid constituents, quercetin and rutin on serum uric acid levels in oxonate-induced mice and xanthine dehydrogenase and xanthine oxidase activities in mouse liver. *Journal of ethnopharmacology*. **2004**, 93, 133-140.
9. D.S. Ghallab, E. Shawky, A.M. Metwally, I. Celik, R.S. Ibrahim, M.M. Mohyeldin. Integrated in silico-in vitro strategy for the discovery of potential xanthine oxidase inhibitors from Egyptian propolis and their

- synergistic effect with allopurinol and febuxostat. *RSC advances* **2022**, 12, 2843-2872.
10. J.U. Song, J.W. Jang, T.H. Kim, H. Park, W.S. Park, S.H. Jung, G.T. Kim. Structure-based design and biological evaluation of novel 2-(indol-2-yl) thiazole derivatives as xanthine oxidase inhibitors. *Bioorganic & medicinal chemistry letters* **2016**, 26, 950-954.
 11. N. Onul, O. Ertik, N. Mermer, R. Yanardag. Synthesis and antioxidant, antixanthine oxidase, and antielastase activities of novel N, substituted polyhalogenated nitrobutadiene derivatives. *Journal of biochemical and molecular toxicology* **2008**, 32, e22021.
 12. V. D. Bock, D. Speijer, H. Hiemstra, J. H. Van Maarseveen. 1, 2, 3-Triazoles as peptide bond isosteres: synthesis and biological evaluation of cyclotetrapeptide mimics. *Organic & biomolecular chemistry* **2017**, 5, 971-975.
 13. N. G. Aher, V. S. Pore, N. N. Mishra, A. Kumar, P. K. Shukla, A. Sharma, M. K. Bhat. Synthesis and antifungal activity of 1,2,3-triazole containing fluconazole analogues. *Bioorg. Med. Chem. Lett.* **2009**, 19, 759.
 14. M. Whiting, J. C. Tripp, Y.-C. Lin, W. Lindstrom, A. J. Olson, J. H. Elder, K. B. Sharpless, Valery V. Fokin. Rapid Discovery and Structure–Activity Profiling of Novel Inhibitors of Human Immunodeficiency Virus Type 1 Protease Enabled by the Copper(I)-Catalyzed Synthesis of 1,2,3-Triazoles and Their Further Functionalization. *J. Med. Chem.* **2006**, 49, 7697-7710.
 15. D. R. Buckle, D. J. Outred, C. J. M. Rockell, H. Smith, B. A.. Studies on v-Triazoles. 7. Antiallergic: 9-Oxo-1ff,9 fi-benzopyrano[2,3-d]-v-triazoles., *J. Med. Chem.* **1983**, 26, 251.
 16. K. Kacprzak. Efficient one-pot synthesis of 1, 2, 3-triazoles from benzyl and alkyl halides *Synlett* **2005**, 36, 943.
 17. X. L. Wang, K. Wan, C. H. Zhou. Synthesis of novel sulfanilamide-derived 1,2,3-triazoles and their evaluation for antibacterial and antifungal activities. *Eur. J. Med. Chem.* **2010**, 45, 4631.
 18. S. R. Patpi, L. Pulipati, P. Yogeewari, D. Sriram, N. Jain, B. Sridhar, R. Murthy, T. Anjana Devi, S. V. Kalivendi, S. Kantavari. Design, Synthesis, and Structure–Activity Correlations of Novel Dibenzo[b,d]furan, Dibenzo[b,d]thiophene, and N-Methylcarbazole Clubbed 1,2,3-Triazoles as Potent Inhibitors of Mycobacterium tuberculosis. *J. Med. Chem.* **2012**, 55, 3911.
 19. M. J. Giffin, H. Heaslet, A. Brik, Y. C. Lin, G. Cauvi, C. H. Wong, D. E. McRee, J. H. Elder, C. D. Stout, B. E. Torbett. Design, Synthesis, and Structure–Activity Correlations of Novel Dibenzo[b,d]furan, Dibenzo[b,d]thiophene, and N-Methylcarbazole Clubbed 1,2,3-Triazoles as Potent Inhibitors of Mycobacterium tuberculosis. *J. Med. Chem.* **2008**, 51, 6263.
 20. S. Zhang, Z. Xu, C. Gao, Q. C. Ren, L. Chang, Z. S. Lv, L. S. Feng. A copper (I)-catalyzed 1, 2, 3-triazole azide–alkyne click compound is a potent inhibitor of a multidrug-resistant HIV-1 protease variant. *Eur. J. Med. Chem.* **2017**, 1938, 501.
 21. Bahuguna, D. S. Rawan. An overview of new antitubercular drugs, drug candidates, and their targets. *Med. Res. Rev.* **2019**, 40, 263.
 22. D. K. Dalvie, A. S. Kalgutkar, S. C. Khojasteh-Bakht, R. S. Obach, J. P. O'Donnell. Biotransformation Reactions of Five-Membered Aromatic Heterocyclic Rings. *Chem. Res. Toxicol.* **2002**, 15, 1269-1299.
 23. Y. L. Angell, K. Burgess. Peptidomimetics via copper-catalyzed azide–alkyne cycloadditions. *Chem. Soc. Rev.* **2007**, 36, 1264-1689
 24. G. Biagi, I. Giorgi, O. Livi, V. Scartoni, I. Tonetti, A. Lucacchini. Xanthine oxidase inhibition: effect of a linear carboalkoxy substituent on C-2 of the nucleus of 8-azahypoxanthine. *ChemInform* **2010**, 22(12), 243-243.
 25. Y. Turkmen, G. Yagiz Erdemir, P.Yuksel Mayda, A. Akdemir, A. Gunaydin Akyildiz, A.Altundas, Synthesis, anti-TB activities, and molecular docking studies of 4-(1,2,3- triazolyl)arylmethanone derivatives. *J. Biochem. Mol. Toxicol.* **2022**, 36, e22998.
 26. P. Y. Wang, H. S. Fang, W. B. Shao, J. Zhou, Z. Chen, B. A. Song, S. Yang. Synthesis and biological evaluation of pyridinium-functionalized carbazole derivatives as promising antibacterial agents. *Bioorganic & medicinal chemistry letters* **2017**, 27, 4294-4297.
 27. J. V. Singh, P. M. S. Bedi, H. Singh, S. Sharma. Xanthine oxidase inhibitors: patent landscape and clinical development (2015–2020). *Expert Opinion on Therapeutic Patents* **2020**, 30, 769-780.
 28. R. Ojha, J. Singh, A. Ojha, H. Singh, S. Sharma, K. Nepali. An updated patent review: xanthine oxidase inhibitors for the treatment of hyperuricemia and gout (2011-2015). *Expert opinion on therapeutic patents* **2017**, 27, 311-345.
 29. B. Sahu, R. Muruganatham, I. N. N. Namboothiri. Synthetic and Mechanistic Investigations on the Rearrangement of 2,3-Unsaturated 1,4-Bis(alkylidene)carbenes to Enediyne. *European Journal of Organic Chemistry* **2007**, 15, 2477-2489.
 30. M. H. Shaikh, D. D. Subhedar, M. Arkile, V. M. Khedkar, N. Jadhav, D. Sarkar, B. B. Shingate. Synthesis and bioactivity of novel triazole incorporated benzothiazinone derivatives as antitubercular and antioxidant agent. *Bioorganic & medicinal chemistry letters* **2016**, 26, 561-569.
 31. G.Y. Erdemir, A. Altundaş A. Synthesis and structure analysis of methyl 1-benzyl-5-(phenylamino)methyl-1H-1,2,3-triazole-4-carboxylate. *Organic communications* **2023**, 16, 46-53.
 32. G.Y. Erdemir, A. Altundaş A. Highly Regioselective One-Step Synthesis Of 1-Benzyl-5-Formyl-1,2,3-Triazole-4-Carboxylates. *Chemistry of Heterocyclic Compounds* **2023**, 59, 267-276.
 33. F. Himo, T. Lovell, R. Hilgraf, V. V. Rostovtsev, L. Noodleman, K.B Sharpless, V.V. Fokin. VV. Copper(I)-catalyzed synthesis of azoles. DFT study predicts unprecedented reactivity and intermediates *Journal of the American Chemical Society* **2005**, 127, 210-216.
 34. Y. Zhang, Z. Zhang, Y. Chen, Y.Li. Copper (II) immobilized on aminated poly (vinyl chloride) as an efficient and retrievable catalyst for the CuAAC reaction in water under mild conditions. *Research on Chemical Intermediates* **2017**, 43, 7307-7318.
 35. R. B. Nasir Baiga, R. S. Varma. Copper on chitosan: a recyclable heterogeneous catalyst for azide–alkyne cycloaddition reactions in water. *Green Chemistry* **2013**, 15, 1839-1843.
 36. N. Joshi, S. Banerjee. PVP coated copper–iron oxide nanocomposite as an efficient catalyst for Click reactions. *Tetrahedron Letters* **2015**, 56, 4163-4169.
 37. Y. Liu, G. Nie, Z. Zhou, L. Jia, and Y. Chen. Copper-catalyzed oxidative cross-dehydrogenative coupling/oxidative cycloaddition: Synthesis of 4-acyl-1, 2, 3-triazoles. *The Jour. of Org. Chem* **2017**, 82, 9198.
 38. O. Trott, A.J. Olson. Improving the speed and accuracy of docking with a new scoring function, efficient optimization and multithreading. *J. Comput. Chem.* **2010**, 31, 455–461.
 39. J. Eberhardt, D. Santos-Martins, A.F. Tillack, S. Forli. AutoDock Vina 1.2.0: New Docking Methods, Expanded Force Field, and Python Bindings. *J. Chem. Inf. Modeling* **2021**, 61, 3891–3898.
 40. Gaussian 09, Revision E.01, Frisch, M. J. Trucks, G. W. Schlegel, H. B. Scuseria, G. E. Robb, M. A. Cheeseman, J. R. Scalmani, G. Barone, V. Mennucci, B. Petersson, G. A. et al. Gaussian, Inc., Wallingford, CT, USA, **2009**.
 41. Y. Rose, J.M. Duarte, R. Lowe, J. Segura, C. Bi, C. Bhikadiya, L. Chen, A.S. Rose, S. Bittrich, S.K. Burley, J.D. Westbrook. RCSB protein data bank: Architectural advances towards integrated searching and efficient access to macromolecular structure data from the PDB archive. *J. Mol. Biol.* **2021**, 433, 166704.
 42. E.F. Pettersen, T.D. Goddard, C.C. Huang, G.S. Couch, D.M. Greenblatt, E.C. Meng, T.E. Ferrin. UCSF Chimera a visualization system for exploratory research and analysis. *J. Comput. Chem.* **2004**, 25, 1605–1612.
 43. Accelrys Software Inc AS. Discovery Studio 3.5. San Diego, CA; **2013**.
 44. D. Ozerkan, O. Ertik, B. Kaya, S. E. Kuruca, R., Yanardag, B. Ülküseven. Novel palladium (II) complexes with tetradentate thiosemicarbazones. Synthesis, characterization, in vitro cytotoxicity and xanthine oxidase inhibition. *Investigational new drugs* **2019**, 37, 1187-1197.
 45. Q. Mao, X. Dai, G. Xu, Y. Su, B. Zhang, D. Liu, S. Wang. Design, synthesis and biological evaluation of 2-(4-alkoxy-3-cyano) phenyl-6-oxo-1, 6-dihydropyrimidine-5-carboxylic acid derivatives as novel

- xanthine oxidase inhibitors. *European journal of medicinal chemistry* **2019**, 181, 111558.
46. Abdussamat Güzel, Samir Abbas Ali Noma, Betül Şen, Ali Kazancı et al. "Synthesis, characterization and inhibitor properties of benzimidazolium salts bearing 4- (methylsulfonyl)benzyl side arms", *Journal of Molecular Structure*, **2023**.
 47. Chadha N, Tiwari AK, Kumar V, Milton MD, Mishra AK. In silico thermodynamics stability change analysis involved in BH4 responsive mutations in phenylalanine hydroxylase: QM/MM and MD simulations analysis. *J Biomol Struct Dyn*. **2015**;33(3):573-83.
 48. R. Rosario, C. Cerchia R. Nasso, V. Romanelli, E. De Vendittis, M. Masullo, A. Lavecchia. Novel Reversible Inhibitors of Xanthine Oxidase Targeting the Active Site of the Enzyme. *Antioxidants* **2023**, 12, 825.
 49. S. Li, Y. Zhang, T. J., Wu, Q. X., Olounfeh, K. M., Zhang, F. H. Meng. Synthesis and biological evaluation of 5-benzyl-3-pyridyl-1H-1, 2, 4-triazole derivatives as xanthine oxidase inhibitors. *Medicinal Chemistry* **2020**, 16, 119-127.
 50. G. Yagiz, S. A. A. Noma, A. Altundas, K. Al-Khafaji, T. Taskin-Tok, B. Ates. Synthesis, inhibition properties against xanthine oxidase and molecular docking studies of dimethyl N-benzyl-1H-1,2,3-triazole-4,5-dicarboxylate and (N-benzyl-1H-1,2,3-triazole-4,5-diyl) dimethanol derivatives. *Bioorganic Chemistry* **2021**, 108, 104654.
 51. K.M. Dawood, M.A. Raslan, A.A. Abbas, B.E. Mohamed, M.H. Abdellattif, M.S. Nafie, M.K. Hassan, Novel Bis-Thiazole Derivatives: Synthesis and Potential Cytotoxic Activity Through Apoptosis with Molecular Docking Approaches, **2021**, 9.
 52. A.O. El-Abd, S.M. Bayomi, A.K. El-Damasy, B. Mansour, N.I. Abdel-Aziz, M.A. El-Sherbeny, Synthesis and Molecular Docking Study of New Thiazole Derivatives as Potential Tubulin Polymerization Inhibitors, *ACS Omega*, **2022**, 7(37), 33599-33613.
 53. R. Matta, J. Pochampally, B.N. Dhoddi, S. Bhokya, S. Bitla, A.G. Akkiraju, Synthesis, antimicrobial and antioxidant activity of triazole, pyrazole containing thiazole derivatives and molecular docking studies on COVID-19, *BMC Chemistry*, **2023**, 17(1), 61.
 54. H.A. Abd El Salam, U. Fathy, E.M. Zayed, M.F. El Shehry, a. Ahmed E.Gouda, Design, Synthesis, Cytotoxic Activity and Molecular Docking Studies of Naphthyl Pyrazolyl Thiazole Derivatives as Anticancer Agents, *ChemistrySelect*, **2023**, 8(2), e202203956.